Comments of reviewer #1

The manuscript presents a comprehensive and theoretically sound investigation into the multi-generation ·OH oxidation mechanisms of styrene. The study employs high-level quantum chemical calculations to elucidate complex reaction pathways, including the formation of bicyclic peroxy radicals (BPR) and their subsequent reactions, which are crucial for understanding SOA formation from aromatic compounds. The topic is of significant interest to the atmospheric chemistry community. While the computational methodology is robust and the overall conclusions are supported by the data, the manuscript requires revisions to improve clarity, depth of discussion, and to address several specific technical points before it can be accepted for publication.

Response: We appreciate the reviewers' comments and have carefully revised the manuscript accordingly. Following is our point-by-point response.

1. please use "OH radical" and "·OH" consistently in the manuscript.

Response: Based on the Reviewer's suggestion, "OH radical" and "·OH" have been used throughout the manuscript.

2. In Page 8, when introducing subscript letters (e.g., S2-1-x) to denote species for the first time, please clearly define their meaning.

Response: Based on the Reviewer's suggestion, the meaning of subscript letter has been explained in the revised manuscript. The peroxyl radicals RO_2 formed from the addition reactions of alkyl radicals R with O_2 have multiple possible conformers due to the different orientation of O_2 attack. In order to distinguish the different conformers in RO_2 radicals, the subscript letter x is used in the present study. The energy ordering of different conformers follows an alphabetical sequence, in which letter a denotes the lowest energy conformer.

Corresponding descriptions have been added in the page 8 line 214-217 of the revised manuscript:

In order to distinguish the different conformers, the subscript letter x is used in the present study. The energy ordering of different conformers follows an alphabetical sequence, in which letter a denotes the lowest energy conformer.

3. In Page 8, Line 216, If ΔE_r > 59.6 kcal/mol, this is an endothermic reaction. Please verify whether this description is correct.

Response: Based on the Reviewer's suggestion, the value of ΔE_r has been corrected in the revised manuscript. The attack of an O_2 molecule on the C-center site of S1-1 leads to the formation of first generation peroxy radicals S2-1-x (ΔE_r > -59.6 kcal/mol).

Corresponding descriptions have been added in the page 8 line 211-213 of the revised manuscript:

The attack of an O_2 molecule on the C-center site of S1-1 leads to the formation of the first generation peroxy radicals S2-1-x (ΔE_r > -59.6 kcal/mol).

4. In Page 9, Line 238, when discussing the pseudo-first-order rate constant for the RO_2 bimolecular reaction, it is recommended that the authors provide additional clarification regarding the typical atmospheric reactant concentration corresponding to the value of ~0.01 s^{-1}. Note that the k value cited in the reference refers to indoor environments.

Response: Based on the Reviewer's suggestion, the relevant descriptions on the pseudo-first-order rate constants for the bimolecular reactions of RO_2 radicals with HO_2 radicals and NO have been added in the revised manuscript. In indoor environments, the concentration of HO_2 radicals is ~24 pptv, which is about half of the concentration of NO (Fu et al., 2024). Previous studies have reported that the rate coefficients $k_{RO2+HO2}$ and k_{RO2+NO} for the reactions of alkyl peroxyl radicals with HO_2 radicals and NO are 1.7×10^{-11} and 9.0×10^{-12} cm^3 $molecule^{-1}$ s^{-1} (Atkinson and Arey, 2003; Boyd et al., 2003), respectively, leading to the pseudo-first-order rate constants $k'_{RO2+HO2} = k_{RO2+HO2}$ [HO_2] and $k'_{RO2+NO} = k_{RO2+NO}$ [NO] of ~0.01 s^{-1} in each case in indoor environments. In the atmosphere, the concentration of HO_2 radicals is 20-40 pptv (Bianchi et al., 2019; Wang et al., 2017), resulting in the pseudo-first-order rate constant $k'_{RO2+HO2}$ of 0.01-0.02 s^{-1}. The isomerization reaction of RO_2 radicals is competitive with the bimolecular reactions with HO_2 radicals only when the rate coefficient of intramolecular H-shifts exceeds 0.01-0.02 s^{-1}. The typical atmospheric concentration of NO is 0.4-40 ppbv (Bianchi et al., 2019; Wang et al., 2017), leading to the pseudo-first-order rate constant k'_{RO2+NO} of 0.1-10 s^{-1}. The intramolecular H-shift reaction of RO_2 radicals can compete with the bimolecular reaction with NO only when the rate coefficient of the former case exceeds 10 s^{-1}. Therefore, we use the

$k'_{RO2+HO2}$ (0.01-0.02 s^{-1}) and k'_{RO2+NO} (0.1-10 s^{-1}) values as thresholds to evaluate the relative importance of the isomerization reactions of RO_2 radicals under the low- and high-NO_x conditions.

Corresponding descriptions have been added in the page 9 line 251-271 of the revised manuscript:

In the low-NO_x conditions, the bimolecular reaction with HO_2 radicals is expected to be the dominant sink for RO_2 radicals (Orlando and Tyndall, 2012; Vereecken et al., 2015). Previous studies have reported that the rate coefficient $k_{RO2+HO2}$ for the reactions of alkyl peroxyl radicals with HO_2 radicals is 1.7 × 10^{-11} cm^3 $molecule^{-1}$ s^{-1} (Atkinson and Arey, 2003; Boyd et al., 2003). The typical atmospheric concentration of HO_2 radicals is 20-40 pptv (Wang et al., 2017; Bianchi et al., 2019), resulting in the pseudo-first-order rate constant $k'_{RO2+HO2}$ = $k_{RO2+HO2}$ [HO_2] of 0.01-0.02 s^{-1}. The isomerization reaction of RO_2 radicals is competitive with the bimolecular reactions with HO_2 radicals only when the rate coefficient of intramolecular H-shifts exceeds 0.01-0.02 s^{-1}. In the high-NO_x conditions, the bimolecular reaction of RO_2 radicals with NO is considered to be a dominant sink (Orlando and Tyndall, 2012; Vereecken et al., 2015). The rate coefficient k_{RO2+NO} for the reaction of alkyl peroxyl radicals with NO is determined to be 9.0 × 10^{-12} cm^3 $molecule^{-1}$ s^{-1} (Atkinson and Arey, 2003; Bianchi et al., 2019). The typical atmospheric concentration of NO is 0.4-40 ppbv (Wang et al., 2017; Wang et al., 2019), leading to the pseudo-first-order rate constant k'_{RO2+NO} = k_{RO2+NO} [NO] of 0.1-10 s^{-1}. The intramolecular H-shift reaction of RO_2 radicals can compete with the bimolecular reaction with NO only when the rate coefficient of the former case exceeds 10 s^{-1}. Therefore, we use the $k'_{RO2+HO2}$ (0.01-0.02 s^{-1}) and k'_{RO2+NO} (0.1-10 s^{-1}) values as thresholds to evaluate the relative importance of the isomerization reactions of RO_2 radicals under the low- and high-NO_x conditions.

5. In Page 11, Line 288, The citation "Zhang et al., 209;" is incomplete and should be corrected to the full and correct reference, which is likely "Zhang et al., 2019".

Response: Based on the Reviewer's suggestion, the related reference has been corrected in the revised manuscript.

6. In Page 11, Lines 279-288, authors attribute the discrepancy between this study and the

results of Zhang et al. (2024) at the ·OH addition sites primarily to the latter's failure to account for pre-reaction complexes. This claim requires further evidence to substantiate. It is recommended to supplement the study with complete potential energy surfaces for the C1 and C6 sites under both methodologies. Based on the calculated energy barriers, the branching ratios for ·OH addition to the C1 and C6 sites at 298 K should be computed.

Response: Based on the Reviewer's suggestion, the energy barriers (ΔE_a) of all the elementary reactions involved in the addition of OH radical to the different sites of 1st-ROOH(S4) are recalculated using the DLPNO-CCSD(T)/aug-cc-pVTZ//M06-2X/6-311+G(d,p) method employed in the Zhang's study (Zhang et al., 2024). The calculated energy barriers are compared with those obtained using the M06-2X/6-311++G (3df,3pd)//M06-2X/6-31+g(d,p) method employed in the present study, as shown in Figure 2 and Table S3. In this work, the *syn*-OH-addition is defined as the scenario in which the addition of OH radical occurs at the same side as the –OOH group, while the *anti*-OH-addition is referred to the scenario in which the addition of OH radical occurs at the opposite side as the –OOH group. For the *syn*-OH-addition reactions, the addition of OH radical to the C1-site of 1st-ROOH (S4) exhibits the lowest barrier (ΔE_a = 3.6 kcal/mol) due to the stability of the formed product, $P_{S4\text{-}add1'}$. A similar conclusion is also obtained from the *anti*-OH-addition reactions that the OH-addition pathway occurring at the C1-site is favorable (ΔE_a = 0.8 kcal/mol). Notably, the preferred OH-addition pathway in the *anti*-OH-addition reactions exhibits greater competitiveness compared to that in the *syn*-OH-addition reactions. It can be explained by the greater steric hindrance present in the latter reaction.

As shown in Table S3, the ΔE_a values obtained using the M06-2X/6-311++G(3df,3pd) method are in good agreement with those derived from the DLPNO-CCSD(T)/aug-cc-pVTZ method. The largest deviation and the average absolute deviation are 1.2 and 0.9 kcal/mol, respectively, indicating that the M06-2X/6-311++G(3df,3pd) method employed in this study is reliable. Based on the values of ΔE_a obtained using the DLPNO-CCSD(T)/ aug-cc-pVTZ method, it can also be concluded that the addition of OH radical to C1-site, occurring at the opposite direction relative to the –OOH group, is energetically favorable. The rate coefficients of the addition of OH radical to the different sites of 1st-ROOH are calculated to be 8.2×10^{-12} (C1-site), 5.8×10^{-15} (C2-site), 8.3×10^{-15} (C3-site), 8.6×10^{-15} (C4-site), 2.7×10^{-12} (C5-site) and $4.1 \times$

10^{-13} (C6-site) cm^3 $molecule^{-1}$ s^{-1}, respectively. The branching ratios for OH addition to the C1, C5 and C6 sites are predicted to be 72.4%, 23.8% and 3.6%, respectively, while the sum of branching ratios for OH addition to other carbon sites is less than 1%.

Our result is opposite to Zhang's finding that the addition of OH radical to C6-site would be the most favorable pathway (Zhang et al., 2024). The discrepancy can be explained by the following three factors: (1) The 1^{st}-ROOH conformer selected in the Zhang's study is not the global minimum. In the present study, the global minimum conformer of 1^{st}-ROOH, identified through the conformer search, is found to be 2.2 kcal/mol in energy lower than the 1^{st}-ROOH structure selected in the Zhang's study (Figure R1). (2) The pre-reactive complexes are not considered in the Zhang's study. The addition of OH radical to C1-, C2-, C3- and C6-sites, occurring at the opposite direction relative to the –OOH group, are merely considered in the Zhang's study. They found that the apparent energy barrier (defined as the energy difference between transition state and reactant) of the addition of OH radical to C6-site is smallest, and is therefore expected to be the favorable pathway. Actually, these OH-addition reactions are modulated by the pre-reactive complexes. It may be inappropriate to determine the favorable pathway based solely on apparent activation energy without considering the pre-reaction complexes. (3) From a geometric perspective, the addition of OH radical to C6-site is associated with greater steric hindrance compared to other sites, as C6-atom connects with a larger functional group. Base on the aforementioned discussions, we believe that the addition of OH radical to C6-site is unlikely to be the dominant pathway. Our calculations also confirm that the addition of OH radical to C6-site is less importance compared to that at the C1-site.

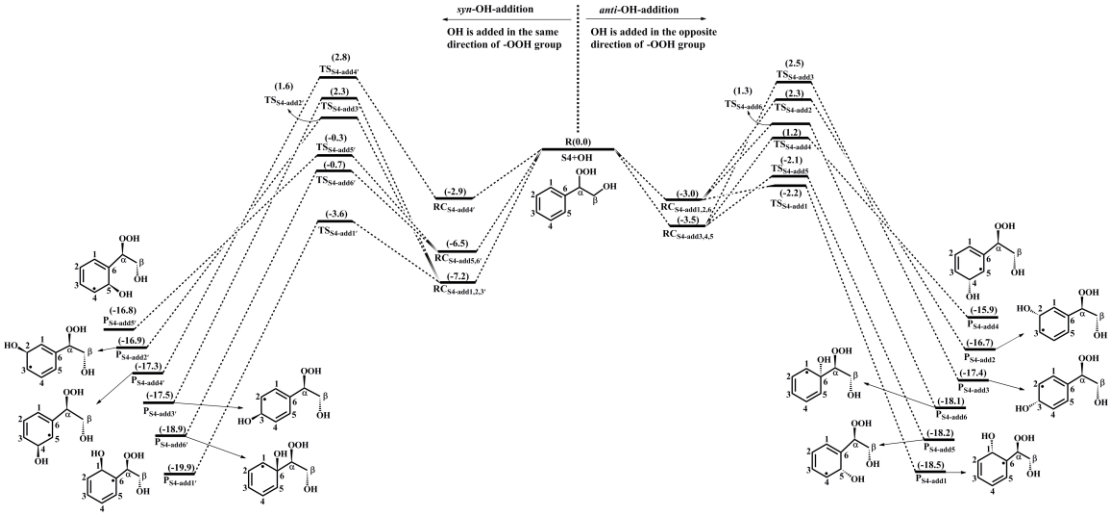

Figure 2. PES for the oxidation of 1st-ROOH(S4) initiated by OH radical at the M06-2X/6-311++G(3df,3pd)//M06-2X/6-31+g(d,p) level

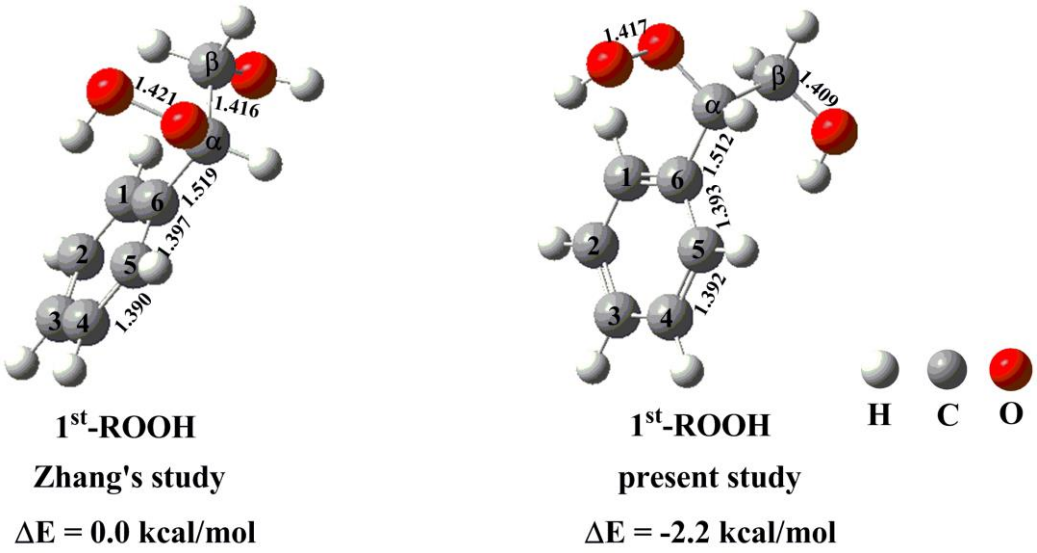

1st-ROOH
Zhang's study
ΔE = 0.0 kcal/mol

1st-ROOH
present study
ΔE = -2.2 kcal/mol

Figure R1. The geometric parameters and the relative energies (Δ*E*) of the hydroperoxide 1st-ROOH selected in the Zhang's study and in the present study

Table S3 The energy barriers (ΔE_a in kcal/mol) of the addition OH radical to the different sites of 1st-ROOH (S4) calculated at the DLPNO-CCSD(T)/aug-cc-pVTZ//M06-2X/6-311+G(d,p) and M06-2X/6-311++G(3df,3pd)//M06-2X/6-31+g(d,p)levels

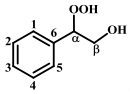 (1st-ROOH (S4))	DLPNO-CCSD(T)/aug-cc-pVTZ// M06-2X/6-311+G(d,p)	M06-2X/6-311++G(3df,3pd)// M06-2X/6-31+g(d,p)
syn-OH-addition (OH is added in the same direction of -OOH group)		
C1-site	3.3	3.6
C2-site	7.8	8.8

C3-site	8.4	9.5
C4-site	5.4	5.7
C5-site	5.0	6.2
C6-site	4.7	5.8
anti-OH-addition (OH is added in the opposite direction of -OOH group)		
C1-site	2.0	0.8
C2-site	6.3	5.3
C3-site	6.7	6.0
C4-site	5.7	4.7
C5-site	2.6	1.4
C6-site	5.2	4.3

Corresponding descriptions have been added in the page 12 line 308-356 of the revised manuscript:

The reaction 1st-ROOH (S4) + OH proceeds through the addition of OH radical to either side of the benzene ring to yield various alkyl radicals, as depicted in Figure 2. In the present study, syn-OH-addition is defined as the scenario in which the addition of OH radical occurs at the same side as the –OOH group, while anti-OH-addition is referred to the scenario in which the addition of OH radical occurs at the opposite side as the –OOH group. For the syn-OH-addition reactions, the addition of OH radical to the C1-site of 1st-ROOH (S4) exhibits the lowest barrier (ΔE_a = 3.6 kcal/mol) due to the stability of the formed product, $P_{S4\text{-}add1'}$. A similar conclusion is also obtained from the anti-OH-addition reactions that the OH-addition pathway occurring at the C1-site is favorable (ΔE_a = 0.8 kcal/mol). Notably, the preferred OH-addition pathway in the anti-OH-addition reactions exhibits greater competitiveness compared to that in the syn-OH-addition reactions. It can be explained by the greater steric hindrance present in the latter reaction. In order to further evaluate the reliability of our results, ΔE_a of all the syn-OH-addition and anti-OH-addition reactions are recalculated using the DLPNO-CCSD(T)/ aug-cc-pVTZ//M06-2X/6-311+G(d,p) method. As shown in Table S3, the ΔE_a values obtained using the M06-2X/6-311++G(3df,3pd) method are in good agreement with those derived from the DLPNO-CCSD(T)/aug-cc-pVTZ method. The largest deviation and the average absolute deviation

are 1.2 and 0.9 kcal/mol, respectively, indicating that the M06-2X/6-311++G(3df,3pd) method employed in this study is reliable. Based on the values of ΔE_a obtained using the DLPNO-CCSD(T)/ aug-cc-pVTZ method, it can also be concluded that the addition of OH radical to C1-site, occurring at the opposite direction relative to the –OOH group, is energetically favorable. The rate coefficients of the addition of OH radical to the different sites of 1st-ROOH are calculated to be 8.2 × 10^{-12} (C1-site), 5.8 × 10^{-15} (C2-site), 8.3 × 10^{-15} (C3-site), 8.6 × 10^{-15} (C4-site), 2.7 × 10^{-12} (C5-site) and 4.1 × 10^{-13} (C6-site) cm^3 $molecule^{-1}$ s^{-1}, respectively. The branching ratios for ·OH addition to the C1, C5 and C6 sites are predicted to be 72.4%, 23.8% and 3.6%, respectively, while the sum of branching ratios for ·OH addition to other carbon sites is less than 1%.

Our result is opposite to Zhang's finding that the addition of OH radical to C6-site would be the most favorable pathway (Zhang et al., 2024). The discrepancy can be explained by the following three factors: (1) The 1st-ROOH conformer selected in the Zhang's study is not the global minimum. In the present study, the global minimum conformer of 1st-ROOH, identified through the conformer search, is found to be 2.2 kcal/mol lower than the 1st-ROOH structure selected in the Zhang's study. (2) The pre-reactive complexes are not considered in the Zhang's study. The addition of OH radical to C1-, C2-, C3- and C6-sites, occurring at the opposite direction relative to the –OOH group, are merely considered in the Zhang's study. They found that the apparent energy barrier of the addition of OH radical to C6-site is smallest, and is therefore expected to be the favorable pathway. Actually, these OH-addition reactions are modulated by the pre-reactive complexes. It may be inappropriate to determine the favorable pathway based solely on apparent activation energy without considering the pre-reaction complexes. (3) From a geometric perspective, the addition of OH radical to C6-site is associated with greater steric hindrance compared to other sites, as C6-atom connects with a larger functional group. Base on the aforementioned discussions, we believe that the addition of OH radical to C6-site is unlikely to be the dominant pathway. Our calculations also confirm that the addition of OH radical to C6-site is less importance compared to that at the C1-site.

7. Why did the author consider only the addition pathway and not the H-abstraction pathway when studying the ·OH oxidation of 2nd-ROOH (S6) and 2nd-RONO2 (S26) in Section 3.3?.

Response: Based on the Reviewer's suggestion, the H-abstraction pathways involved in the oxidation of 2^{nd}-ROOH (S6) and 2^{nd}-$RONO_2$ (S26) initiated by OH radical have been added in the revised manuscript. OH-initiated oxidation of 2^{nd}-ROOH (S6) can either undergo through the addition of OH radical to either side of the C_3=C_4 double bond to generate the alkyl radicals, or proceed via H-abstraction from the different carbon sites to produce the alkyl radicals and alkoxyl radicals, as shown in Figures S16 and S17. For the OH-addition reactions, *syn*-OH-addition is defined as the addition of OH radical on the same side as the –OOH group, while *anti*-OH-addition is referred to the addition of OH radical on the opposite side as the –OOH group. The addition of OH radical to the C3-site of the C_3=C_4 double bond forming the product $P_{S6\text{-}abs3}$ has the smallest barrier (ΔE_a = 2.4 kcal/mol) and the exoergicity of -33.5 kcal/mol. For the H-abstraction reactions, the abstraction of hydrogen atom at the C_5-site is the most favorable pathway (ΔE_a = 3.6 kcal/mol) and the exoergicity of -20.2 kcal/mol. It is mainly because that the presence of an allyl group enhances the stability of the resulting product $P_{S6\text{-}abs5}$. Notably, the abstraction of hydrogen atom at the C_2-site proceeds through a concerted process of C_2-H bond and bridge O-O bond rupture, leading to the formation of an alkoxyl radical $P_{S6\text{-}abs2}$ (ΔE_a = 7.2 kcal/mol). This reaction is expected to be less importance due to its higher energy barrier. The rate coefficient of the favorable OH-addition reaction is calculated to be 6.4×10^{-11} cm^3 $molecule^{-1}$ s^{-1}, which is about one order of magnitude greater than that of the preferable H-abstraction reaction (4.1×10^{-12} cm^3 $molecule^{-1}$ s^{-1}). Based on the above discussion, it can be concluded that OH-addition reaction is favorable on both thermochemically and kinetically. This conclusion is further supported by the OH + alkene reaction systems that OH-addition pathways are predominant (Yang et al., 2017; Chen et al., 2021; Arathala et al., 2024).

OH-initiated oxidation of 2^{nd}-$RONO_2$ (S26) includes four different OH-addition pathways and five different H-abstraction pathways, as displayed in Figures S19 and S20. For the OH-addition reactions, the attack of OH radical on the C3-site of the C_3=C_4 double bond forming the product $P_{S26\text{-}add3}$, occurring on the same direction relative to the –ONO_2 group, is found to be the favorable pathway (ΔE_a = 2.4 kcal/mol, ΔE_r = -33.6 kcal/mol). For the H-abstraction reactions, the abstraction of hydrogen atom at the C5-site is identified as the preferable pathway (ΔE_a = 5.7 kcal/mol, ΔE_r = -20.1 kcal/mol) due to the enhanced stability of the resulting product $P_{S26\text{-}add5}$ by the presence of an allyl group. By comparing the values of ΔE_a and ΔE_r of the favorable

OH-addition and H-abstraction pathways, it can concluded that the former case is dominant on both thermochemically and kinetically. This conclusion is consistent with the result from the reaction 2nd-ROOH (S6) + OH that OH-addition is more competitive than H-abstraction.

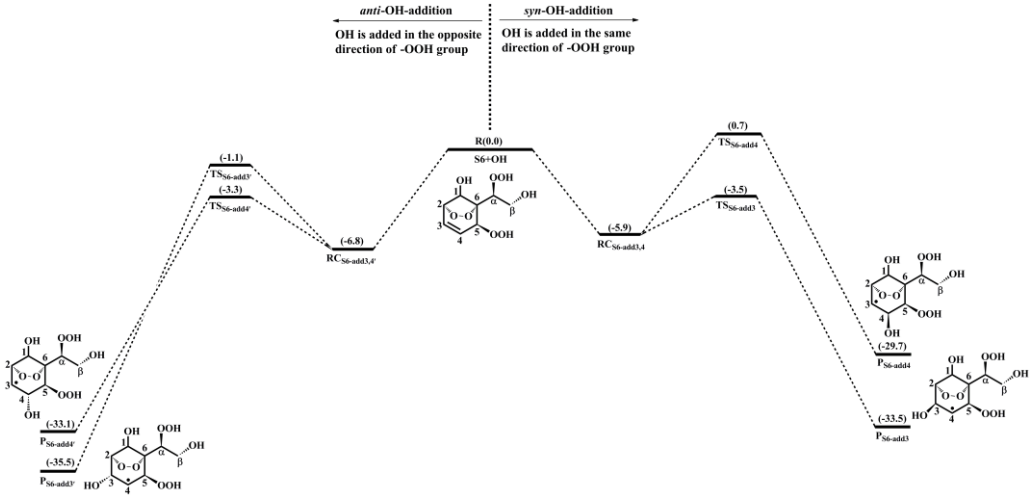

Figure S16. PES for the OH-addition reactions involved in the OH-initiated oxidation of 2nd-ROOH (S6) at the M06-2X/6-311++G(3df,3pd)//M06-2X/6-31+g(d,p) level

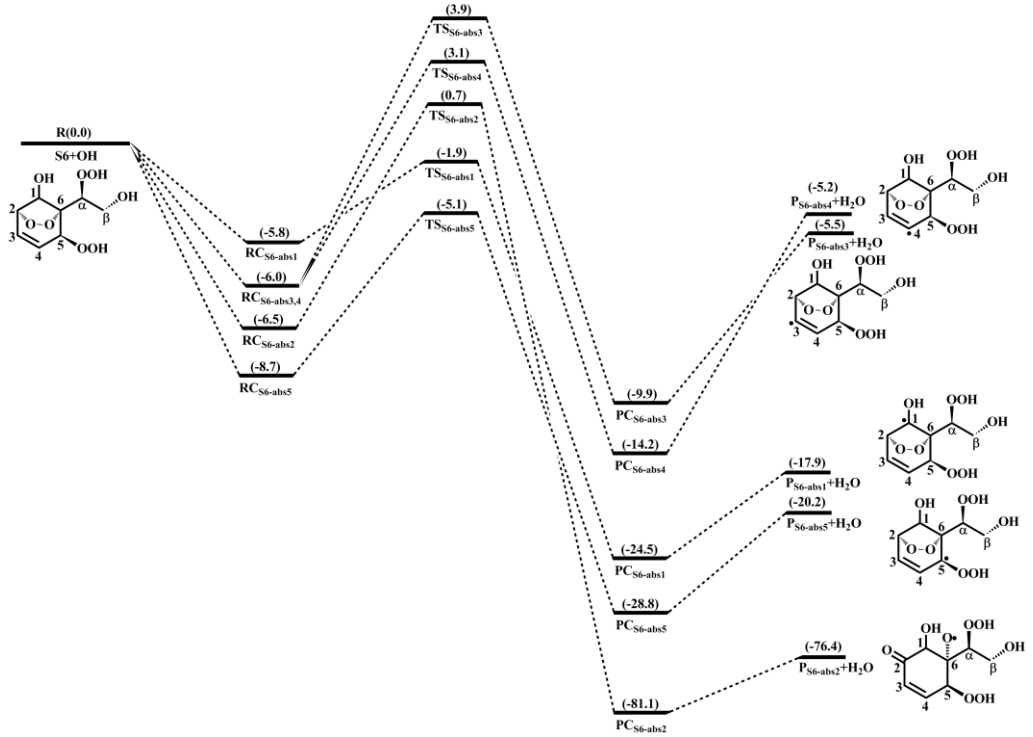

Figure S17. PES for the H-abstraction reactions involved in the OH-initiated oxidation of 2nd-ROOH (S6) at the M06-2X/6-311++G(3df,3pd)//M06-2X/6-31+g(d,p) level

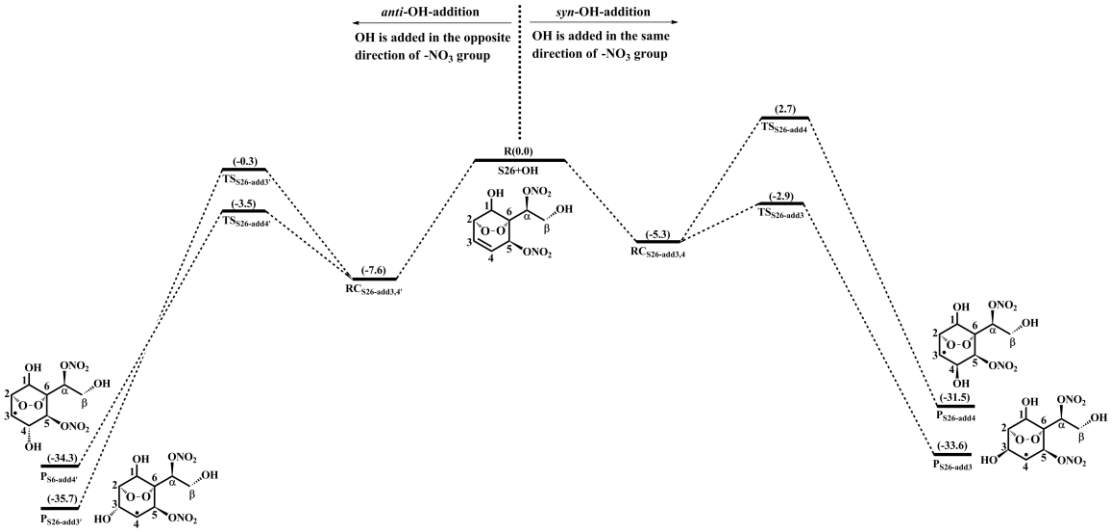

Figure S19. PES for the OH-addition reactions involved in the OH-initiated oxidation of 2nd-$RONO_2$ (S26) at the M06-2X/6-311++G(3df,3pd)//M06-2X/6-31+g(d,p) level

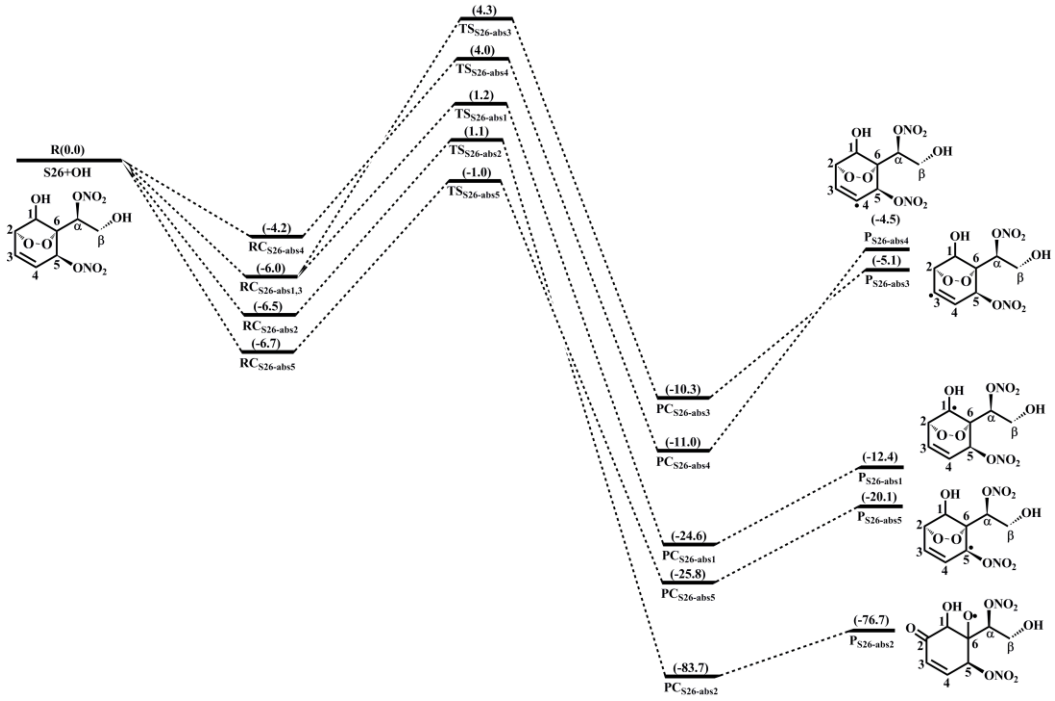

Figure S20. PES for the H-abstraction reactions involved in the OH-initiated oxidation of 2nd-$RONO_2$ (S26) at the M06-2X/6-311++G(3df,3pd)//M06-2X/6-31+g(d,p) level

Corresponding descriptions have been added in the page 23 line 589-611 and page 25 line 646-658 of the revised manuscript:

OH-initiated oxidation of 2nd-ROOH (S6) can either undergo through the addition of OH radical to either side of the C_3=C_4 double bond to generate the alkyl radicals, or proceed via H-abstraction from the different carbon sites to produce the alkyl radicals and alkoxyl radicals, as shown in Figures S16 and S17. For the OH-addition reactions, syn-OH-addition is defined as the

addition of OH radical on the same side as the –OOH group, while anti-OH-addition is referred to the addition of OH radical on the opposite side as the –OOH group. The addition of OH radical to the C3-site of the C_3=C_4 double bond forming the product $P_{S6\text{-}abs3}$ has the smallest barrier (ΔE_a = 2.4 kcal/mol) and the exoergicity of -33.5 kcal/mol. For the H-abstraction reactions, the abstraction of hydrogen atom at the C5-site is the most favorable pathway (ΔE_a = 3.6 kcal/mol) and the exoergicity of -20.2 kcal/mol. It is mainly because that the presence of an allyl group enhances the stability of the resulting product $P_{S6\text{-}abs5}$. Notably, the abstraction of hydrogen atom at the C2-site proceeds through a concerted process of C_2-H bond and -O-O- bridge bond rupture, leading to the formation of an alkoxyl radical $P_{S6\text{-}abs2}$ (ΔE_a = 7.2 kcal/mol). This reaction is expected to be less importance due to its higher energy barrier. The rate coefficient of the favorable OH-addition reaction is calculated to be 6.4 × 10^{-11} cm^3 $molecule^{-1}$ s^{-1}, which is about one order of magnitude greater than that of the preferable H-abstraction reaction (4.1 × 10^{-12} cm^3 $molecule^{-1}$ s^{-1}). Based on the above discussion, it can be concluded that OH-addition reaction is favorable on both thermochemically and kinetically. This conclusion is further supported by the OH + alkene reaction systems that OH-addition pathways are predominant (Chen et al., 2021; Yang et al., 2017; Arathala and Musah, 2024).

OH-initiated oxidation of 2^{nd}-$RONO_2$ (S26) includes four different OH-addition pathways and five different H-abstraction pathways, as displayed in Figures S19 and S20. For the OH-addition reactions, the attack of OH radical on the C3-site of the C_3=C_4 double bond forming the product $P_{S26\text{-}add3}$, occurring on the same direction relative to the –ONO_2 group, is found to be the favorable pathway (ΔE_a = 2.4 kcal/mol, ΔE_r = -33.6 kcal/mol). For the H-abstraction reactions, the abstraction of hydrogen atom at the C5-site is identified as the preferable pathway (ΔE_a = 5.7 kcal/mol, ΔE_r = -20.1 kcal/mol) due to the enhanced stability of the resulting product $P_{S26\text{-}add5}$ by the presence of an allyl group. By comparing the values of ΔE_a and ΔE_r of the favorable OH-addition and H-abstraction pathways, it can concluded that the former case is dominant on both thermochemically and kinetically. This conclusion is consistent with the result from the reaction 2^{nd}-ROOH (S6) + OH that OH-addition is more competitive than H-abstraction.

Reference

Arathala, P., and Musah, R. A.: Atmospheric chemistry of chloroprene initiated by OH radicals: combined Ab initio/DFT calculations and kinetics analysis, J. Phys. Chem. A, 128, 8983-8995, https://doi.org/10.1021/acs.jpca.4c05428, 2024.

Atkinson, R., and Arey, J.: Atmospheric degradation of volatile organic compounds, Chem. Rev., 103, 4605-4638, https://doi.org/10.1021/cr0206420, 2003.

Bianchi, F., Kurtén, T., Riva, M., Mohr, C., Rissanen, M. P., Roldin, P., Berndt, T., Crounse, J. D., Wennberg, P. O., Mentel, T. F., Wildt, J., Junninen, H., Jokinen, T., Kulmala, M., Worsnop, D. R., Thornton, J. A., Donahue, N., Kjaergaard, H. G., and Ehn, M.: Highly oxygenated organic molecules (HOM) from gas-phase autoxidation involving peroxy radicals: a key contributor to atmospheric aerosol, Chem. Rev., 119, 3472-3509, https://doi.org/10.1021/acs.chemrev.8b00395, 2019.

Boyd, A. A., Flaud, P. M., Daugey, N., and Lesclaux, R.: Rate constants for RO_2 + HO_2 reactions measured under a large excess of HO_2, J. Phys. Chem. A, 107, 818-821, https://doi.org/10.1021/jp026581r, 2003.

Chen, L., Huang, Y., Xue, Y., Jia, Z., and Wang, W.: Atmospheric oxidation of 1-butene initiated by OH radical: Implications for ozone and nitrous acid formations, Atmos. Environ., 244, 118010-118021, https://doi.org/10.1016/j.atmosenv.2020.118010, 2021.

Fu, Z., Guo, S., Xie, H. B., Zhou, P., Boy, M., Yao, M., and Hu, M.: A near-explicit reaction mechanism of chlorine-initiated limonene: implications for health risks associated with the concurrent use of cleaning agents and disinfectants, Environ. Sci. Technol., 58, 19762-19773, https://doi.org/10.1021/acs.est.4c04388, 2024.

Wang, S., Wu, R., Berndt, T., Ehn, M., and Wang, L.: Formation of highly oxidized radicals and multifunctional products from the atmospheric oxidation of alkylbenzene, Environ. Sci. Technol., 51, 8442-8449, https://doi.org/10.1021/acs.est.7b02374, 2017.

Yang, F., Deng, F., Pan, Y., Zhang, Y., Tang, C., and Huang, Z.: Kinetics of hydrogen abstraction and addition reactions of 3-hexene by OH radicals, J. Phys. Chem. A, 121, 1877-1889, https://doi.org/10.1021/acs.jpca.6b11499, 2017.

Zhang, H., Wang, J., Dong, B., Xu, F., Liu, H., Zhang, Q., Zong, W., and Shi, X.: New mechanism for the participation of aromatic oxidation products in atmospheric nucleation, Sci. Total Environ., 917, 170487-170494, https://doi.org/10.1016/j.scitotenv.2024.170487, 2024.